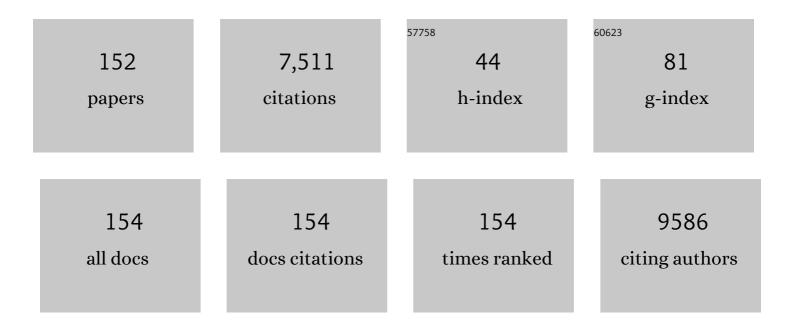
Zhongyuan Liu

List of Publications by Year in descending order

Source: https://exaly.com/author-pdf/5077065/publications.pdf Version: 2024-02-01



ZHONCYUAN LUL

#	Article	IF	CITATIONS
1	Ultrahard nanotwinned cubic boron nitride. Nature, 2013, 493, 385-388.	27.8	662
2	Nanotwinned diamond with unprecedented hardness and stability. Nature, 2014, 510, 250-253.	27.8	611
3	Investigation on Microwave Absorption Properties for Multiwalled Carbon Nanotubes/Fe/Co/Ni Nanopowders as Lightweight Absorbers. Journal of Physical Chemistry C, 2011, 115, 14025-14030.	3.1	448
4	Flexible Allâ€Solidâ€State Supercapacitors based on Liquidâ€Exfoliated Blackâ€Phosphorus Nanoflakes. Advanced Materials, 2016, 28, 3194-3201.	21.0	290
5	Teâ€Doped Black Phosphorus Fieldâ€Effect Transistors. Advanced Materials, 2016, 28, 9408-9415.	21.0	241
6	Microwave Absorption Properties of CoS ₂ Nanocrystals Embedded into Reduced Graphene Oxide. ACS Applied Materials & Interfaces, 2017, 9, 28868-28875.	8.0	215
7	Hardness of covalent compounds: Roles of metallic component and d valence electrons. Journal of Applied Physics, 2008, 104, .	2.5	166
8	Liquidâ€Exfoliated Black Phosphorous Nanosheet Thin Films for Flexible Resistive Random Access Memory Applications. Advanced Functional Materials, 2016, 26, 2016-2024.	14.9	161
9	Controlled Incorporation of Ni(OH) ₂ Nanoplates Into Flowerlike MoS ₂ Nanosheets for Flexible Allâ€Solidâ€State Supercapacitors. Advanced Functional Materials, 2014, 24, 6700-6707.	14.9	145
10	Enhanced laser scribed flexible graphene-based micro-supercapacitor performance with reduction of carbon nanotubes diameter. Carbon, 2014, 75, 236-243.	10.3	139
11	Nonvolatile Ferroelectric Memory Effect in Ultrathin αâ€In ₂ Se ₃ . Advanced Functional Materials, 2019, 29, 1808606.	14.9	137
12	Broadband Black Phosphorus Optical Modulator in the Spectral Range from Visible to Midâ€Infrared. Advanced Optical Materials, 2015, 3, 1787-1792.	7.3	115
13	Fabrication of carbon encapsulated Co 3 O 4 nanoparticles embedded in porous graphitic carbon nanosheets for microwave absorber. Carbon, 2015, 89, 372-377.	10.3	114
14	Fabrication of NiCo ₂ -Anchored Graphene Nanosheets by Liquid-Phase Exfoliation for Excellent Microwave Absorbers. ACS Applied Materials & Interfaces, 2017, 9, 12673-12679.	8.0	111
15	Compressed glassy carbon: An ultrastrong and elastic interpenetrating graphene network. Science Advances, 2017, 3, e1603213.	10.3	110
16	Enhanced stability of black phosphorus field-effect transistors with SiO ₂ passivation. Nanotechnology, 2015, 26, 435702.	2.6	102
17	Blackâ€Phosphorusâ€Incorporated Hydrogel as a Conductive and Biodegradable Platform for Enhancement of the Neural Differentiation of Mesenchymal Stem Cells. Advanced Functional Materials, 2020, 30, 2000177.	14.9	100
18	Microwave Synthesized Three-dimensional Hierarchical Nanostructure CoS2/MoS2 Growth on Carbon Fiber Cloth: A Bifunctional Electrode for Hydrogen Evolution Reaction and Supercapacitor. Electrochimica Acta, 2016, 212, 941-949.	5.2	93

#	Article	IF	CITATIONS
19	Sulfur-Doped Black Phosphorus Field-Effect Transistors with Enhanced Stability. ACS Applied Materials & Interfaces, 2018, 10, 9663-9668.	8.0	93
20	Enhanced Photoresponse of SnSe-Nanocrystals-Decorated WS ₂ Monolayer Phototransistor. ACS Applied Materials & Interfaces, 2016, 8, 4781-4788.	8.0	91
21	Flexible Black-Phosphorus Nanoflake/Carbon Nanotube Composite Paper for High-Performance All-Solid-State Supercapacitors. ACS Applied Materials & Interfaces, 2017, 9, 44478-44484.	8.0	89
22	First-principles studies of structural and electronic properties of hexagonalBC5. Physical Review B, 2006, 73, .	3.2	75
23	Microwave absorption properties of multiwalled carbon nanotube/FeNi nanopowders as light-weight microwave absorbers. Journal of Magnetism and Magnetic Materials, 2013, 343, 281-285.	2.3	74
24	Approaching diamond's theoretical elasticity and strength limits. Nature Communications, 2019, 10, 5533.	12.8	73
25	Enhanced thermoelectric figure of merit in nanocrystalline Bi2Te3 bulk. Journal of Applied Physics, 2009, 105, .	2.5	71
26	Two-dimensional materials and one-dimensional carbon nanotube composites for microwave absorption. Nanotechnology, 2018, 29, 025704.	2.6	71
27	Atomically Resolving Polymorphs and Crystal Structures of In ₂ Se ₃ . Chemistry of Materials, 2019, 31, 10143-10149.	6.7	71
28	Carbon-Encapsulated Co 3 O 4 @CoO@Co Nanocomposites for Multifunctional Applications in Enhanced Long-life Lithium Storage, Supercapacitor and Oxygen Evolution Reaction. Electrochimica Acta, 2016, 220, 322-330.	5.2	68
29	Lateral Bilayer MoS ₂ –WS ₂ Heterostructure Photodetectors with High Responsivity and Detectivity. Advanced Optical Materials, 2019, 7, 1900815.	7.3	65
30	Twoâ€Dimensionalâ€Germanium Phosphideâ€Reinforced Conductive and Biodegradable Hydrogel Scaffolds Enhance Spinal Cord Injury Repair. Advanced Functional Materials, 2021, 31, 2104440.	14.9	65
31	Microwave synthesized self-standing electrode of MoS 2 nanosheets assembled on graphene foam for high-performance Li-Ion and Na-Ion batteries. Journal of Alloys and Compounds, 2016, 660, 11-16.	5.5	64
32	Gate tunable MoS ₂ –black phosphorus heterojunction devices. 2D Materials, 2015, 2, 034009.	4.4	61
33	Gate tunable WSe ₂ –BP van der Waals heterojunction devices. Nanoscale, 2016, 8, 3254-3258.	5.6	60
34	Mechanical properties of nanocrystalline TiC–ZrC solid solutions fabricated by spark plasma sintering. Ceramics International, 2014, 40, 10517-10522.	4.8	57
35	SnS 2 Nanoflakes Anchored Graphene obtained by Liquid Phase Exfoliation and MoS 2 Nanosheet Composites as Lithium and Sodium Battery Anodes. Electrochimica Acta, 2017, 227, 203-209.	5.2	57
36	Atomic-Scale Observation of Reversible Thermally Driven Phase Transformation in 2D In ₂ Se ₃ . ACS Nano, 2019, 13, 8004-8011.	14.6	57

#	Article	IF	CITATIONS
37	Orthogonal Electric Control of the Outâ€Ofâ€Plane Fieldâ€Effect in 2D Ferroelectric αâ€In ₂ Se ₃ . Advanced Electronic Materials, 2020, 6, 2000061.	5.1	56
38	Sodium-Induced Reordering of Atomic Stacks in Black Phosphorus. Chemistry of Materials, 2017, 29, 1350-1356.	6.7	55
39	Degradation of black phosphorus: a real-time ³¹ P NMR study. 2D Materials, 2016, 3, 035025.	4.4	53
40	Prediction of a sandwichlike conducting superhard boron carbide: First-principles calculations. Physical Review B, 2006, 73, .	3.2	48
41	Direct Observation of Room-Temperature Dislocation Plasticity in Diamond. Matter, 2020, 2, 1222-1232.	10.0	48
42	Great thermoelectric power factor enhancement of CoSb3 through the lightest metal element filling. Applied Physics Letters, 2011, 98, .	3.3	47
43	Application of hard ceramic materials B4C in energy storage: Design B4C@C core-shell nanoparticles as electrodes for flexible all-solid-state micro-supercapacitors with ultrahigh cyclability. Nano Energy, 2020, 75, 104947.	16.0	47
44	Compressive Strength of Diamond from First-Principles Calculation. Journal of Physical Chemistry C, 2010, 114, 17851-17853.	3.1	46
45	Bulk Re ₂ C: Crystal Structure, Hardness, and Ultra-incompressibility. Crystal Growth and Design, 2010, 10, 5024-5026.	3.0	46
46	Photodetectors based on sensitized two-dimensional transition metal dichalcogenides—A review. Journal of Materials Research, 2017, 32, 4115-4131.	2.6	46
47	Facile synthesis and excellent electrochemical performance of CoP nanowire on carbon cloth as bifunctional electrode for hydrogen evolution reaction and supercapacitor. Science China Materials, 2017, 60, 1179-1186.	6.3	42
48	Grain-boundary-rich polycrystalline monolayer WS2 film for attomolar-level Hg2+ sensors. Nature Communications, 2021, 12, 3870.	12.8	42
49	Chalcopyrite polymorph for superhard BC2N. Applied Physics Letters, 2006, 89, 151911.	3.3	41
50	Superior microwave absorption properties of ultralight reduced graphene oxide/black phosphorus aerogel. Nanotechnology, 2018, 29, 235604.	2.6	41
51	Highly sensitive and fast monolayer WS ₂ phototransistors realized by SnS nanosheet decoration. Nanoscale, 2017, 9, 1916-1924.	5.6	39
52	Structure and mechanical properties of osmium carbide: First-principles calculations. Applied Physics Letters, 2008, 93, .	3.3	38
53	2D Hybrid Superlattice-Based On-Chip Electrocatalytic Microdevice for <i>in Situ</i> Revealing Enhanced Catalytic Activity. ACS Nano, 2020, 14, 1635-1644.	14.6	36
54	Two-dimensional black phosphorous induced exciton dissociation efficiency enhancement for high-performance all-inorganic CsPbI ₃ perovskite photovoltaics. Journal of Materials Chemistry A, 2019, 7, 22539-22549.	10.3	35

#	Article	IF	CITATIONS
55	Well-controlled Core-shell structures based on Fe3O4 nanospheres coated by polyaniline for highly efficient microwave absorption. Applied Surface Science, 2022, 591, 153176.	6.1	35
56	Chemical Vapor Synthesized WS2-Embedded Polystyrene-derived Porous Carbon as Superior Long-term Cycling Life Anode Material for Li-ion Batteries. Electrochimica Acta, 2015, 153, 49-54.	5.2	33
57	Narrowing Working Voltage Window to Improve Layered GeP Anode Cycling Performance for Lithium-Ion Batteries. ACS Applied Materials & Interfaces, 2020, 12, 17466-17473.	8.0	33
58	A tetragonal phase of superhard BC2N. Journal of Applied Physics, 2009, 105, .	2.5	32
59	Liquid-exfoliation of S-doped black phosphorus nanosheets for enhanced oxygen evolution catalysis. Nanotechnology, 2019, 30, 035701.	2.6	32
60	Porous bismuth antimony telluride alloys with excellent thermoelectric and mechanical properties. Journal of Materials Chemistry A, 2021, 9, 4990-4999.	10.3	32
61	Microwave synthesis of SnS2 nanoflakes anchored graphene foam for flexible lithium-ion battery anodes with long cycling life. Materials Letters, 2016, 174, 24-27.	2.6	31
62	Microwave absorption characteristics of CH3NH3PbI3 perovskite/carbon nanotube composites. Journal of Materials Science, 2017, 52, 13023-13032.	3.7	31
63	Metallic layered germanium phosphide GeP ₅ for high rate flexible all-solid-state supercapacitors. Journal of Materials Chemistry A, 2018, 6, 19409-19416.	10.3	31
64	Metal–organic framework derived cobalt phosphosulfide with ultrahigh microwave absorption properties. Nanotechnology, 2018, 29, 405703.	2.6	30
65	Direct large-scale fabrication of C-encapsulated B4C nanoparticles with tunable dielectric properties as excellent microwave absorbers. Carbon, 2019, 148, 504-511.	10.3	30
66	Fabrication of multifunctional carbon encapsulated Ni@NiO nanocomposites for oxygen reduction, oxygen evolution and lithium-ion battery anode materials. Science China Materials, 2017, 60, 947-954.	6.3	29
67	Enhanced thermoelectric performance of Na-doped PbTe synthesized under high pressure. Science China Materials, 2018, 61, 1218-1224.	6.3	29
68	Spark plasma sintering of the nonstoichiometric ultrafine-grained titanium carbides with nano superstructural domains of the ordered carbon vacancies. Materials Chemistry and Physics, 2011, 130, 352-360.	4.0	28
69	Superstructural nanodomains of ordered carbon vacancies in nonstoichiometric ZrC _{0.61} . Journal of Materials Research, 2012, 27, 1230-1236.	2.6	28
70	Large and Anisotropic Linear Magnetoresistance in Single Crystals of Black Phosphorus Arising From Mobility Fluctuations. Scientific Reports, 2016, 6, 23807.	3.3	26
71	Ultrahigh-Gain and Fast Photodetectors Built on Atomically Thin Bilayer Tungsten Disulfide Grown by Chemical Vapor Deposition. ACS Applied Materials & Interfaces, 2017, 9, 42001-42010.	8.0	26
72	Ambipolar Photoresponsivity in an Ultrasensitive Photodetector Based on a WSe ₂ /InSe Heterostructure by a Photogating Effect. ACS Applied Materials & Interfaces, 2021, 13, 50213-50219.	8.0	26

#	Article	IF	CITATIONS
73	Facile-synthesized carbonaceous photonic crystals/magnetic particle nanohybrids with heterostructure as an excellent microwave absorber. Journal of Alloys and Compounds, 2018, 741, 814-820.	5.5	25
74	Microwave absorbing properties of two dimensional materials GeP5 enhanced after annealing treatment. Applied Physics Letters, 2019, 114, .	3.3	24
75	Multistate Logic Inverter Based on Black Phosphorus/SnSeS Heterostructure. Advanced Electronic Materials, 2019, 5, 1800416.	5.1	24
76	Proximity Enhanced Hydrogen Evolution Reactivity of Substitutional Doped Monolayer WS ₂ . ACS Applied Materials & Interfaces, 2021, 13, 19406-19413.	8.0	24
77	Microwave absorption properties of heterostructure composites of two dimensional layered magnetic materials and graphene nanosheets. Applied Physics Letters, 2019, 115, .	3.3	23
78	Siliconâ€Phosphorusâ€Nanosheetsâ€Integrated 3Dâ€Printable Hydrogel as a Bioactive and Biodegradable Scaffold for Vascularized Bone Regeneration. Advanced Healthcare Materials, 2022, 11, e2101911.	7.6	23
79	Passively Q-switched ytterbium-doped ScBO ₃ laser with black phosphorus saturable absorber. Optical Engineering, 2016, 55, 081312.	1.0	21
80	Role of plastic deformation in tailoring ultrafine microstructure in nanotwinned diamond for enhanced hardness. Science China Materials, 2017, 60, 178-185.	6.3	21
81	Large topological Hall effect in nonchiral hexagonal MnNiGa films. Applied Physics Letters, 2017, 110, .	3.3	21
82	Photoluminescence and Raman Spectra Oscillations Induced by Laser Interference in Annealing reated Monolayer WS ₂ Bubbles. Advanced Optical Materials, 2019, 7, 1801373.	7.3	21
83	Intensive suppression of thermal conductivity in Nd0.6Fe2Co2Sb12-xGex through spontaneous precipitates. Journal of Applied Physics, 2013, 114, 083715.	2.5	20
84	Novel three-dimensional boron nitride allotropes from compressed nanotube bundles. Journal of Materials Chemistry C, 2014, 2, 7022.	5.5	20
85	Carbonaceous photonic crystals as ultralong cycling anodes for lithium and sodium batteries. Journal of Materials Chemistry A, 2015, 3, 13786-13793.	10.3	19
86	Enhanced Stability of Black Phosphorus Fieldâ€Effect Transistors via Hydrogen Treatment. Advanced Electronic Materials, 2018, 4, 1700455.	5.1	19
87	Magnetic Anisotropy Control with Curie Temperature above 400 K in a van der Waals Ferromagnet for Spintronic Device. Advanced Materials, 2022, 34, e2201209.	21.0	19
88	Enhanced electromagnetic wave absorption properties of NiCo2 nanoparticles interspersed with carbon nanotubes. Journal of Magnetism and Magnetic Materials, 2019, 471, 185-191.	2.3	18
89	Synergistic Additiveâ€Assisted Growth of 2D Ternary In ₂ SnS ₄ with Giant Gateâ€Tunable Polarizationâ€Sensitive Photoresponse. Small, 2021, 17, e2008078.	10.0	18
90	Scalable Van der Waals Encapsulation by Inorganic Molecular Crystals. Advanced Materials, 2022, 34, e2106041.	21.0	18

#	Article	lF	CITATIONS
91	Formation, structure, and electric property of CaB4 single crystal synthesized under high pressure. Applied Physics Letters, 2010, 96, .	3.3	17
92	High pressure synthesis of Te-doped CoSb3 with enhanced thermoelectric performance. Journal of Materials Science: Materials in Electronics, 2015, 26, 385-391.	2.2	17
93	Strain Release Induced Novel Fluorescence Variation in CVD-Grown Monolayer WS ₂ Crystals. ACS Applied Materials & Interfaces, 2017, 9, 34071-34077.	8.0	17
94	Layered porous materials indium triphosphide InP3 for high-performance flexible all-solid-state supercapacitors. Journal of Power Sources, 2019, 438, 227010.	7.8	17
95	Highâ€Performance Broadband Photodetectors of Heterogeneous 2D Inorganic Molecular Sb ₂ O ₃ /Monolayer MoS ₂ Crystals Grown via Chemical Vapor Deposition. Advanced Optical Materials, 2020, 8, 2000168.	7.3	17
96	Coexistence of multiple metastable polytypes in rhombohedral bismuth. Scientific Reports, 2016, 6, 20337.	3.3	16
97	Si ₁₀ : A sp ³ Silicon Allotrope with Spirally Connected Si ₅ Tetrahedrons. Chemistry of Materials, 2016, 28, 6441-6445.	6.7	16
98	C ₆₀ on Nanostructured Nb-Doped SrTiO ₃ (001) Surfaces. Journal of Physical Chemistry C, 2010, 114, 3416-3421.	3.1	15
99	Low-Temperature Diffusion of Oxygen through Ordered Carbon Vacancies in Zr2Cx: The Formation of Ordered Zr2CxOy. Inorganic Chemistry, 2012, 51, 5164-5172.	4.0	15
100	{111}-specific twinning structures in nonstoichiometric ZrC _{0.6} with ordered carbon vacancies. Journal of Applied Crystallography, 2013, 46, 43-47.	4.5	15
101	Improved photoresponse and stable photoswitching of tungsten disulfide single-layer phototransistor decorated with black phosphorus nanosheets. Journal of Materials Science, 2017, 52, 11506-11512.	3.7	15
102	Facile Synthesis of Carbon-Encapsulated Ni Nanoparticles Embedded into Porous Graphite Sheets as High-Performance Microwave Absorber. ACS Sustainable Chemistry and Engineering, 2018, 6, 16179-16185.	6.7	15
103	Mechanical Robustness Two-Dimensional Silicon Phosphide Flake Anodes for Lithium Ion Batteries. ACS Sustainable Chemistry and Engineering, 2020, 8, 17597-17605.	6.7	15
104	Annealing-Induced {011}-Specific Cyclic Twins in Tetragonal Zirconia Nanoparticles. Journal of Physical Chemistry C, 2012, 116, 21052-21058.	3.1	14
105	Interlayer exchange coupling and magnetic reversal in Co/Pt multilayers. Journal of Magnetism and Magnetic Materials, 2013, 325, 117-121.	2.3	14
106	Grain wall boundaries in centimeter-scale continuous monolayer WS ₂ film grown by chemical vapor deposition. Nanotechnology, 2018, 29, 255705.	2.6	14
107	New hexagonal boron nitride polytypes with triple-layer periodicity. Journal of Applied Physics, 2017, 121, .	2.5	13
108	Simple preparation and excellent microwave attenuation property of Fe3O4- and FeS2- decorated graphene nanosheets by liquid-phase exfoliation. Journal of Alloys and Compounds, 2019, 810, 151881.	5.5	13

#	Article	IF	CITATIONS
109	One-step growth of wafer-scale monolayer tungsten disulfide via hydrogen sulfide assisted chemical vapor deposition. Applied Physics Letters, 2019, 115, .	3.3	13
110	Photodetection application of one-step synthesized wafer-scale monolayer MoS2 by chemical vapor deposition. 2D Materials, 2020, 7, 025020.	4.4	13
111	High-sensitivity and versatile plasmonic biosensor based on grain boundaries in polycrystalline 1L WS2 films. Biosensors and Bioelectronics, 2021, 194, 113596.	10.1	13
112	Synthesis of B–C–N nanocrystalline particle by mechanical alloying and spark plasma sintering. Journal of Materials Science, 2006, 41, 8352-8355.	3.7	12
113	Deep melting reveals liquid structural memory and anomalous ferromagnetism in bismuth. Proceedings of the National Academy of Sciences of the United States of America, 2017, 114, 3375-3380.	7.1	12
114	One-Step Growth of Spatially Graded Mo _{1–<i>x</i>} W _{<i>x</i>} S ₂ Monolayers with a Wide Span in Composition (from <i>x</i> = 0 to 1) at a Large Scale. ACS Applied Materials & Interfaces, 2019, 11, 20979-20986.	8.0	12
115	First-Principles Investigation of Dense B ₄ C ₃ . Journal of Physical Chemistry C, 2007, 111, 13679-13683.	3.1	11
116	Metastable adaptive orthorhombic martensite in zirconia nanoparticles. Journal of Applied Crystallography, 2014, 47, 684-691.	4.5	11
117	Pressure Effect on Order–Disorder Ferroelectric Transition in a Hydrogen-Bonded Metal–Organic Framework. Journal of Physical Chemistry Letters, 2020, 11, 9566-9571.	4.6	11
118	The rise of plastic deformation in boron nitride ceramics. Science China Materials, 2021, 64, 46-51.	6.3	11
119	In Situ Grown Ultrafine RuO ₂ Nanoparticles on GeP ₅ Nanosheets as the Electrode Material for Flexible Planar Micro-Supercapacitors with High Specific Capacitance and Cyclability. ACS Applied Materials & Interfaces, 2021, 13, 47560-47571.	8.0	11
120	Distinct C60 growth modes on anthracene carboxylic acid templates. Applied Physics Letters, 2010, 96, 143115.	3.3	10
121	Tian et al. reply. Nature, 2013, 502, E2-E3.	27.8	10
122	Multifunctional Photodetectors Based on Nanolayered Black Phosphorus/SnS _{0.5} Se _{1.5} Heterostructures. ACS Applied Nano Materials, 2019, 2, 3548-3555.	5.0	10
123	High-performance flexible all-solid-state micro-supercapacitors based on two-dimensional InSe nanosheets. Journal of Power Sources, 2021, 482, 228987.	7.8	10
124	Extreme mechanical anisotropy in diamond with preferentially oriented nanotwin bundles. Proceedings of the National Academy of Sciences of the United States of America, 2021, 118, .	7.1	10
125	Magnetoresistance and Anomalous Hall Effect with Pt Spacer Thickness in the Spin-Valve Co/Pt/[Co/Pt]2 Multilayers. Journal of Superconductivity and Novel Magnetism, 2017, 30, 533-538.	1.8	9
126	Accelerated Degradation of CrCl ₃ Nanoflakes Induced by Metal Electrodes: Implications for Remediation in Nanodevice Fabrication. ACS Applied Nano Materials, 2019, 2, 1597-1603.	5.0	9

#	Article	IF	CITATIONS
127	Prediction of a conducting hard ductile cubic IrC. Physica Status Solidi - Rapid Research Letters, 2010, 4, 230-232.	2.4	8
128	Strengthening in high-pressure quenched Zr. High Pressure Research, 2017, 37, 278-286.	1.2	8
129	Two-dimensional layered materials InSe nanoflakes/carbon nanotubes composite for flexible all-solid-state supercapacitors. Journal of Materials Science, 2020, 55, 2947-2957.	3.7	7
130	Influence of van der Waals epitaxy on phase transformation behaviors in 2D heterostructure. Applied Physics Letters, 2020, 116, .	3.3	7
131	Carbonaceous photonic crystals prepared by high-temperature/hydrothermal carbonization as high-performance microwave absorbers. Journal of Materials Science, 2019, 54, 14343-14353.	3.7	6
132	Recent advances in exchange bias of layered magnetic FM/AFM systems. Science China: Physics, Mechanics and Astronomy, 2013, 56, 61-69.	5.1	5
133	Weak antilocalization effect in exfoliated black phosphorus revealed by temperature- and angle-dependent magnetoconductivity. Journal of Physics Condensed Matter, 2018, 30, 085703.	1.8	5
134	Hydrogen Bond Tuning of Magnetoelectric Coupling in Metal–Organic Frameworks. Journal of Physical Chemistry C, 2020, 124, 16111-16115.	3.1	5
135	Broadband light absorption and photoresponse enhancement in monolayer WSe2 crystal coupled to Sb2O3 microresonators. Nano Research, 2022, 15, 4653-4660.	10.4	5
136	Ferroelectrics: Nonvolatile Ferroelectric Memory Effect in Ultrathin αâ€ i n 2 Se 3 (Adv. Funct. Mater.) Tj ETQq0 0	0 rgBT /O 14.9	verlock 10 Tf
137	Direct one-step synthesis of CoFex@Co@C hybrids derived from a metal organic framework for a lightweight and high-performance microwave absorber. Nanotechnology, 2020, 31, 095703.	2.6	4
138	Peculiar spectra and photocurrent oscillation caused by laser interference in WX2 (X = S, Se) bubbles. Journal of Materials Science, 2020, 55, 15857-15866.	3.7	4
139	Nonlinear optical response of a monolayer WS ₂ and the application of a hundred-MHz nanosecond laser. Optics Express, 2021, 29, 36634.	3.4	4
140	Pressure Control of the Structure and Multiferroicity in a Hydrogen-Bonded Metal–Organic Framework. Inorganic Chemistry, 0, , .	4.0	4
141	Pressure effect on spin-driven multiferroicity in a Y-type hexaferrite. Journal of Materials Chemistry C, 2019, 7, 4173-4177.	5.5	3
142	Magnetism and microwave absorption properties of two-dimensional layered ferromagnetic metal Fe3GeTe2. Journal of Materials Science, 2021, 56, 16524-16532.	3.7	3
143	Current-induced torques in black phosphorus/permalloy bilayers due to crystal symmetry. Applied Physics Letters, 2020, 117, 062403.	3.3	2
144	Controllable growth of multilayered XSe ₂ (X = W and Mo) for nonlinear optical and optoelectronic applications. 2D Materials, 2022, 9, 015012.	4.4	2

#	Article	IF	CITATIONS
145	Heat Treatment Effect on the Magnetic Properties of Cu-Nb Micro-Composites. IEEE Transactions on Applied Superconductivity, 2012, 22, 6002004-6002004.	1.7	1
146	Carbon Vacancy Ordered Non-Stoichiometric ZrC0.6. , 2013, , 478-508.		1
147	Chemical synthesis and characterization of MnO ₂ -coated Co nanoparticles. Journal of Materials Research, 2010, 25, 1748-1754.	2.6	0
148	Chemical synthesis and characterization of manganese oxide coated Ni particles. Science China: Physics, Mechanics and Astronomy, 2013, 56, 1508-1513.	5.1	0
149	n -Dependent variations of coercivity with temperature in [Co/Pt] n multilayers. Applied Surface Science, 2015, 345, 182-186.	6.1	0
150	Photoemission oscillation in epitaxially grown van der Waals β-In ₂ Se ₃ WS ₂ heterobilayer bubbles*. Chinese Physics B, 2021, 30, 117901.	1.4	0
151	Carbon Vacancy Ordered Non-Stoichiometric ZrC0.6. , 0, , 667-689.		0
152	Scalable Van der Waals Encapsulation by Inorganic Molecular Crystals (Adv. Mater. 7/2022). Advanced Materials, 2022, 34, .	21.0	0